H. FU, B. XU, Q. XIAO, S. LI, X. ZHANG, S. BIAN, T. KANG

ISSN 0543-5846
METABK 59(2) 163-166 (2020)
UDC – UDK 669.15/621-41:621.791.057/620.1:537.3:531.79:620.16=111

EFFECT OF CURRENT INTENSITY ON RESIDUAL STRESS OF Q345/2Cr13 DISSIMILAR STEEL PLATES

Received – Primljeno: 2019-08-28
Accepted – Prihvaćeno: 2019-11-15
Original Scientific Paper – Izvorni znanstveni rad

Based on the software Visual-Environment, Finite element method (FEM) was performed on the dissimilar butt-joint between Q345 and 2Cr13 steel aiming at the welding residual stress. The main contents in the paper were different current intensity was applied to modeling the welding process of Q345/2Cr13 dissimilar steel and the law of residual stress field were discussed. Based on the result, different current intensities have little effect on the lateral residual stress, while the longitudinal residual stress and the initial and end of the weld have a great influence. The physical properties of the dissimilar plates lead to uneven distribution of residual stress, and the current intensity should be smaller.

Keywords: steel plates, dissimilar steel welding, current intensity, numerical simulation, residual stress

INTRIDUCTION

With the advancement of science and technology and the development of modern industry, people have put forward higher requirements for the comprehensive performance of welded components [1]. Therefore, in various modern engineering structures, the welding of dissimilar steel has received more attention [2]. The transient stress generated during the welding process and the residual stress formed by the completely cooled after welding lead to uneven distribution of the residual stress of the entire workpiece after welding, and the residual stress affects the working strength of the welded component to some extent [3]. In dissimilar plate welding, the difference in physical properties, chemical properties and tissue composition between metal materials results in a large difference in soldering to the same material [4]. Mainly, there are four differences: the chemical composition of the fusion zone of dissimilar materials is not uniform which carbon migration occurs in the joint fusion zone [5]; the metallographic structure of the welded joints of dissimilar materials is uneven, and it is easy to produce weld cracks and brittle fractures, especially the coarse grain in the fusion zone, which becomes the weakest area of dissimilar metal welded joints [6]; the grain in the heat-affected zone is relatively coarse, and its composition and properties are not uniform, resulting in a significant decrease in the ductility and toughness of the heat-affected zone [7]; the heat-affected zone is also the main part of stress concentration, and its stress-strain distribution is uneven, which is easy to produce welding residual stress and welding deformation after welding [8,9]. Therefore, the residual stress distribution after welding of dissimilar plates has important research significance, and the welding numerical simulation technology allows people to better predict and control the welding residual stress [10-12].

In this paper, the variation of temperature field and strain field of Q345/2Cr13 dissimilar steel during welding is analyzed by changing the welding current intensity. The purpose of this paper is to analyze the variation behavior of Q345/2Cr13 dissimilar steel welding residual stress and provide theoretical guidance for actual welding engineering.

Experimental process

In this paper, the model-meshing software visual-mesh in visual-environment is used to establish the model and mesh. There are two 50 mm × 200 mm × 4 mm plates were built by visual-mesh, and the welding model of the plate is established. The schematic diagram of the model is shown in Figure 1, in which the weld width is set to 5 mm. Plate 1 is low alloy steel Q345, plate 2 is martensitic stainless steel 2Cr13, and the filling material of the weld is 2Cr13. The chemical composition of the two materials is shown in Table 1.

Keep the voltage constant and change the current intensity to change the heat input acting on the unit length of the weld:

$$q_w = g/v$$

Where: q_w is the effective power of the arc; v is the welding speed.

H. Fu, B. Xu (e-mail: boxuchina@163.com), College of Metallurgy and Energy, North China University of Science and Technology, Tangshan, Hebei, China
Q. Xiao, S. Li (e-mail: lishengli@ustl.edu.cn), Key Laboratory of metallurgical engineering, University of Science and Technology Liaoning, Anshan, Liaoning, X. Zhang, S. Bian, China
T. Kang, 725 Research Institute of China Shipbuilding Heavy Industry Group Corporation, China

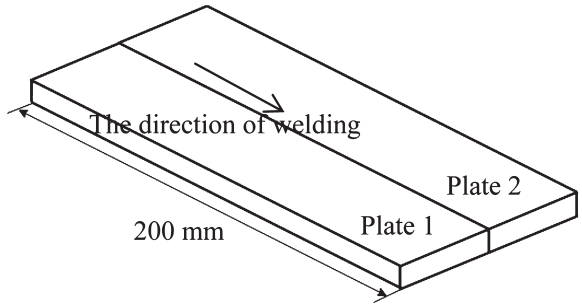

Figure 1 Model schematic

Table1 Chemical **composition of Q345 and 2Cr13**

	C	Si	Mn	Cr
Q345	0,12 - 0,18	0,5	1,7	0,30
2Cr13	0,16 - 0,25	1,0	043	0,12 - 0,14
Mo	V	Ni	S	P
0,10	0,15	0,5	0,045	0,050
-	-	0,60	0,030	0,010

The experimental scheme uses three different current intensities for numerical simulation. The specific welding parameters are shown in Table 2. The speed of welding is 5 mm in each case.

Table 2 **Numerical simulation projects**

Computing scheme	Amp / A	Vol / V	Line power / (J / mm)
Case 1	140	15	294
Case 2	150	15	315
Case 3	160	15	336

The welding process includes many complex physical and chemical metallurgical phenomena such as heat conduction, convection, radiation, evaporation and melt solidification [13,14]. Therefore, the following assumptions are made in the numerical simulation process [15]:

1) Assume that surface deformation does not change heat transfer and mass transfer between the welding arc and the workpiece.
2) Ignore the fuzzy area where the solid-liquid two phases coexist in the molten pool.

Simulation results and analysis

Figure 2 shows the lateral residual stress distribution at different current intensities. It can be seen from the figure that the residual stresses in the three cases in the central weld zone are approximately the same. The lateral stress distribution in the figure shows a certain irregularity. The direct cause of the lateral residual stress is the lateral contraction of the workpiece. The indirect cause is the longitudinal contraction of the workpiece. Under the action of the lateral contraction and longitudinal contraction of the workpiece, the stress distribution is certain irregularity. In addition, it can be seen that the residual stress of the heat affected zone of the panel 1 is less than the residual stress of the panel 2, and

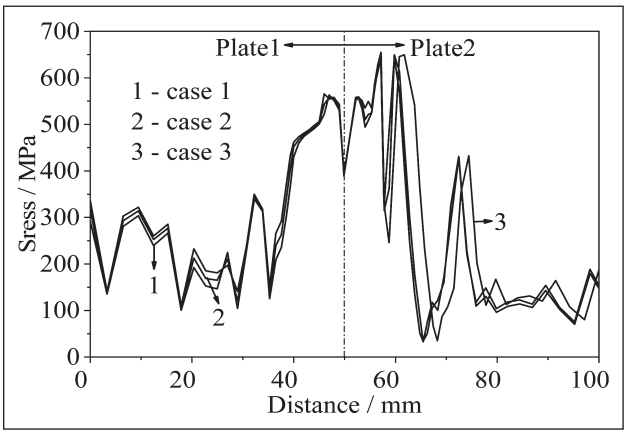

Figure 2 Lateral residual stress comparison

the edge portion of the panel 1 is significantly smaller than the residual stress of the panel 2.This is mainly due to the fact that during the welding process, the material properties of the two plates are different and the heat transfer is inconsistent. The comparison shows that as the current intensity increases, the lateral residual stress increases, but the growth rate is not obvious. Therefore, the change in current intensity has little effect on the lateral residual stress.

Figure 3 shows the residual stress distribution at the weld position at different current intensities. By comparison, it can be found that the residual stress at the weld position is approximately the same, and the increase of the current intensity leads to a small increase in the residual stress of the weld. At the welding start end and the arc end, the longitudinal residual stress gradient is large. This is caused by the arc being unstable in arcing and arcing, and the instability of the arc causes uneven stress distribution at the beginning and end of the welding. The residual stress curves at the middle of the weld at the three current intensities are relatively straight, indicating that the stress distribution in the middle of the weld is uniform and the arc is stable. It can be seen that different current intensities have little effect on the residual stress distribution at the weld.

Figure 4(a) and (b) shows the longitudinal residual stress distribution in the heat-affected zone of the two plates at different current intensities. By comparison, it

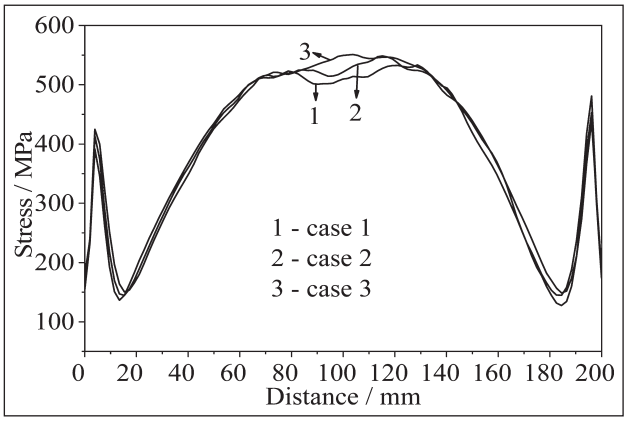

Figure 3 Weld residual stress

is known that, similar to the residual stress distribution at the weld, the longitudinal residual stress gradient is large at the welding start end and the arc end. By calculating the average post-weld residual stress in the welding stabilization stage, the residual stress at the current intensity of 140 A on plate 1 is 488,54 MPa, 150 A is 491,77 MPa, and 160 A is 493,24 MPa, which is 0,67 % and 0,92 % larger than 140 A, respectively. The residual stress of plate 2 at 140 A is 586,41 MPa, 150 A is 614,87 MPa, and 160 A is 636,62 MPa, which is 4,85 % and 8,56 % larger than 140 A, respectively. It is found that the longitudinal residual stress in the heat-affected zone is asymmetrically distributed on both sides of the weld line, and the stress gradient on the side of the 2Cr13 base metal is larger than that on the Q345 base material side, indicating that the welding temperature field is the main factor determining the welding stress field. The thermal conductivity of 2Cr13 is small, resulting in a large temperature gradient, and the yield strength of 2Cr13 is large, resulting in a large residual stress amplitude after welding, indicating that the yield strength is the main factor affecting the residual stress amplitude, which explain that yield strength is the main factor affecting the magnitude of residual stress. At 160 A, the residual stress after welding is large, while at 140 A, the residual stress after welding is the smallest, and the welding process is also stable. Therefore, for the welding of Q345/2Cr13 dissimilar steel, it is better to use smaller current strength welding in terms of reducing residual stress.

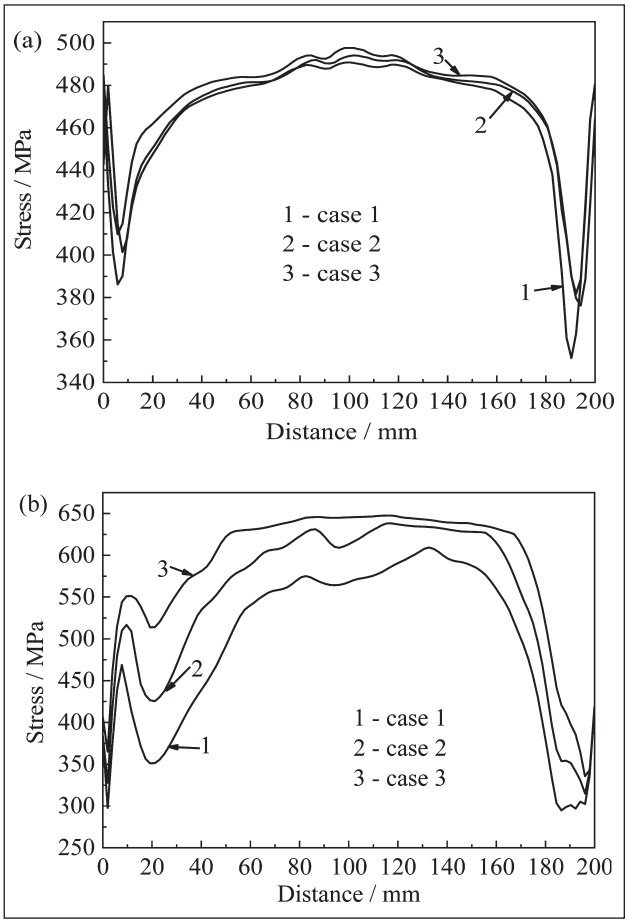

Figure 4 Longitudinal residual stress of Plate1 and Plate2 (a) plate1; (b) plate2

SUMMARY

The change in current intensity results in a change in the weld line energy, but has little effect on the lateral residual stress distribution during the dissimilar plate welding process.

The thermal conductivity and yield strength of the material are the main factors affecting the post-weld residual stress. Leading to dissimilar plate welding, different current intensity has a great influence on the residual stress of the heat affected zone, there is a certain residual stress amplitude difference, and Q345 is obviously smaller than 2Cr13.

For Q345/2Cr13 dissimilar steel welding, in order to reduce residual stress after welding, a small current intensity should be used when the voltage is constant.

Acknowledgments

This work was financially supported by Opening Fund for National Key Laboratory of Metallic Materials for Marine Equipment and Application (SKLMEA-K201801), Liaoning Province Natural Science Fund Project (201602385), 2017 Provincial Key Laboratory Opening Project of Liaoning University of Science and Technology (USTLKFSY201709), Liaoning Provincial Department of Education Innovation Team Project (LT2016003)

REFERENCES

[1] M. A. Derakhshi, J. Kangazian, M. Shamanian. Electron beam welding of inconel 617 to AISI 310: Corrosion behavior of weld metal [J], Vacuum 161 (2019), 371 - 374.

[2] K. L. Wu, X. J. Yuan, T. Lia, et al. Effect of ultrasonic vibration on TIG welding–brazing joining of aluminum alloy to steel [J], Journal of Materials Processing Tech 266 (2019), 230 - 238.

[3] N. Sayyar, M. Shamanian, B. Niroumand. Arc weldability of Incoloy 825 to AISI 321 stainless steel welds [J], Journal of Materials Processing Tech 262 (2018), 562 - 570.

[4] J. Tomków, G. Rogalski, D. Fydrych. Improvement of S355G10+N steel weldability in water environment by Temper Bead Welding [J], Journal of Materials Processing Tech 262 (2018), 372 - 381.

[5] D. Akbari, I. S. Far. Effect of welding heat input on residual stress in butt-welds of dissimilar pipe joints [J], International Journal of Pressure Vessels and Piping 86 (2009), 769 - 776.

[6] N. Kumar, M. Mukherjee, A. Bandyopadhyay, et al. Comparative study of pulsed Nd: YAG laser welding of AISI 304 and AISI 316 stainless steels [J], Optics & Laser Technology 88 (2017), 24 - 39.

[7] S. H. Chen, L. Q. Li, Y. B. Chen, et al. Joining mechanism of Ti/Al dissimilar alloys during laser welding-brazing process [J], Journal of Alloys and Compounds 509 (2011) 3, 891 - 898.

[8] H. M. Soltani, M. Tayebi. Comparative study of AISI 304L to AISI 316L stainless steels joints by TIG and Nd: YAG laser welding [J], Journal of Alloys and Compounds 767 (2018), 112 - 121.
[9] V. M. V. Prasad, V. M. J. Varghese, M. R. Suresh, et al. 3D simulation of residual stress developed during TIG welding of stainless steel pipes [J], Procedia Technology 24 (2016), 364 - 371.
[10] G. D. Q. Caetano, C. C. Silva, M. F. Motta, et al. Influence of rotation speed and axial force on the friction stir welding of AISI 410S ferritic stainless steel [J], Journal of Materials Processing Tech 262 (2018), 430 - 436.
[11] R. Bendikiene, S. Baskutis, J. Baskutiene, et al. Comparative study of TIG welded commercially pure titanium [J], Journal of Manufacturing Processes 36 (2018), 155 - 163.
[12] B. Wu, B. Wang, X. T. Zhao, et al. Effect of active fluxes on thermophysical properties of 309L stainless-steel welds [J], Journal of Materials Processing Tech 255 (2018), 212 - 218.
[13] X. G. Li, B. M. Gong, C. Y. Deng, et al. Effect of pre-strain on microstructure and hydrogen embrittlement of K-TIG welded austenitic stainless steel [J], Corrosion Science 149 (2019), 1 - 17.
[14] Y. F. Zhang, J. H. Huang, Z. Cheng, et al. Study on MIG-TIG double-sided arc welding-brazing of aluminum and stainless steel [J], Materials Letters 172(2016), 146 - 148.
[15] M. Aissani, S. Guessasma, A. Zitouni, et al. Three-dimensional simulation of 304L steel TIG welding process: Contribution of the thermal flux [J], Applied Thermal Engineering 89 (2015), 822 - 832.

Note: Q. H. Xiao is responsible for English language, Liaoning, China